ORIGINAL ARTICLE

Cancer Science WILEY

PTGER3 knockdown inhibits the vulnerability of triple-negative breast cancer to ferroptosis

Song Wang[1] | Yueyao Zhang[1] | Dan Zhang[1] | Jie Meng[1] | Na Che[1,2] | Xiulan Zhao[1,2] | Tieju Liu[1,2]

[1]Department of Pathology, Tianjin Medical University, Tianjin, China

[2]Department of Pathology, Tianjin Medical University General Hospital, Tianjin, China

Correspondence
Tieju Liu and Xiulan Zhao, Department of Pathology, Tianjin Medical University, Qixiangtai Road No. 22, HePing District, Tianjin 300070, China.
Email: liutieju@tmu.edu.cn and zhaoxiulan@tmu.edu.cn

Abstract

Prostaglandin E receptor 3 (PTGER3) is involved in a variety of biological processes in the human body and is closely associated with the development and progression of a variety of cancer types. However, the role of PTGER3 in triple-negative breast cancer (TNBC) remains unclear. In the present study, low PTGER3 expression was found to be associated with poor prognosis in TNBC patients. PTGER3 plays a crucial role in regulating TNBC cell invasion, migration, and proliferation. Upregulation of PTGER3 weakens the epithelial–mesenchymal phenotype in TNBC and promotes ferroptosis both in vitro and in vivo by repressing glutathione peroxidase 4 (GPX4) expression. On the other hand, downregulation of PTGER3 inhibits ferroptosis by increasing GPX4 expression and activating the PI3K-AKT pathway. Upregulation of PTGER3 also enhances the sensitivity of TNBC cells to paclitaxel. Overall, this study has elucidated critical pathways in which low PTGER3 expression protects TNBC cells from undergoing ferroptosis, thereby promoting its progression. PTGER3 may thus serve as a novel and promising biomarker and therapeutic target for TNBC.

KEYWORDS
ferroptosis, GPX4, PI3K-AKT, PTGER3, triple-negative breast cancer

1 | INTRODUCTION

Triple-negative breast cancer (TNBC) is defined as a breast cancer subtype with negative expression of estrogen receptor (ER), progesterone receptor (PR), and human epidermal growth factor receptor-2 (HER2).[1] Patients with TNBC have shorter survival compared with those with other breast cancer subtypes.[2] TNBC is challenging to treat due to poor cell differentiation, molecular heterogeneity, and rapid metastasis, often leading to chemoresistance and recurrence of the disease.[3]

The protein encoded by PTGER3 is a member of the G-protein-coupled receptor family and is one of four receptor types identified

---

for prostaglandin E2 (PGE2).[4] All four receptor types are expressed in breast cancer, but each plays a different role in the development of this disease.[5] In sporadic breast cancer, expression of the PTGER3-encoded EP3 receptor is an important prognostic factor for improved progression-free survival and overall survival (OS).[6] PTGER3 expression also has a significant positive effect on the prognosis of unifocal breast cancer.[7] However, so far there have been few studies on the effect of PTGER3 on the progression of TNBC.

Ferroptosis is a type of cell death caused by iron-dependent lipid peroxidation and the overproduction of reactive oxygen species (ROS). Ferroptosis is a new type of programmed cell death that is different to apoptosis, necrosis, and autophagy in terms of its morphology, biochemistry, and genetics.[8] Research has shown that mesenchymal and de-differentiated cancer cells, as well as treatment-resistant cancer cells, are highly susceptible to inducers of ferroptosis.[9–11] Intracellular metabolic processes determine the sensitivity of cancer cells to ferroptosis,[12] including energy and lipid metabolism.[13] TNBC cells exhibit unique metabolic states for iron and glutathione (GSH) homeostasis, making them more susceptible to ferroptosis than other breast cancer subtypes.[14] Acyl-coenzyme A (CoA) synthetase long-chain family member 4 (Acsl4) is preferentially expressed in TNBC and is closely associated with sensitivity to ferroptosis.[15] Indeed, ferroptosis nanomedicine has been used to improve the therapeutic effect against TNBC.[16] These studies suggest that targeting of ferroptosis may be a promising therapeutic strategy for TNBC.

2 | MATERIALS AND METHODS

2.1 | Cell culture and lentivirus infection

Breast adenocarcinoma cell lines (MDA-MB-231, MDA-MB-453, and MCF-7) were purchased from Shanghai FuHeng Biotechnology Co. Ltd. All cell lines were authenticated during the preceding 3 years using short tandem repeat profiling. They were screened using a Mycoplasma Detection Kit (Lonza, AG), and all experiments were performed with mycoplasma-free cells. Cells were cultured in DMEM supplemented with 10% fetal bovine serum (Hyclone) and 1% penicillin/streptomycin and grown in a humidified 5% CO_2 atmosphere at 37°C. PTGER3 overexpression, shPTGER3 (sh1-PTGER3, sh2-PTGER3, and sh3-PTGER3), and negative control plasmids were constructed by GeneCopoeia and transfected into MDA-MB-231 and MCF-7 cells using lentivirus packaging kits. The shRNA target sequence was GCAGAAAGAATGCAACTTCTT for sh1-PTGER3, CCTGCTGTTAAGAAAGATCCT for sh2-PTGER3, and CCTATCTCATTATCTAATGAA for sh3-PTGER3.

2.2 | Western blot

Proteins were extracted with sodium dodecyl sulfate (SDS) lysis buffer, separated by SDS-PAGE, and then transferred to PVDF membranes. After blocking with 5% skim milk for 1 h, membranes were incubated overnight at 4°C with primary antibody and then for 2 h with secondary antibody. An enhanced chemiluminescence kit (Advansta) was used to detect immunoreactive bands. GAPDH (1:1000 dilution, sc-47724, Santa Cruz) was used as the protein loading control. The following primary antibodies were used: PTGER3 (1:900 dilution, MAB102431-SP) from Novus, Vimentin (1:1000, ab92547) from Abcam, phospho-AKT (S473) (1:500, T40067F) from Abmart, GPX4 (1:1000, #DF6701) and AKT (1:500, #AF6259) from Affinity, E-cadherin (1:1000, #3195) from Cell Signaling Technology, RIPK1 (1:900, 17519-1-AP), and MMP-2 (1:500, 10373-2-AP) from Proteintech.

2.3 | Wound-healing assay

Cells (6×10^4) were seeded in six-well plates and grown until 90% confluence. Scratches of uniform width were made with a sterilized tip. Wound healing at 0, 24, and 48 h was photographed with a Nikon Eclipse TS100 microscope.

2.4 | Cell migration and invasion assay

Cells (4×10^4) in 200 μL of serum-free DMEM were seeded into upper transwell chambers, while 500 μL of medium containing 5% FBS was added to the lower chambers. Transwell chambers included 20 μL of Matrigel for the invasion experiments. Migration assays were performed after 24 h of incubation, and invasion assays after 48 h of incubation. Cold methanol was used to fix the cells, followed by staining with crystal violet for 30 min. Imaging was performed using a Nikon Eclipse TS100 microscope.

2.5 | Colony formation assay

Cells (500 cells/well) were seeded in six-well plates, and adherent cells were grown in DMEM at 37°C for 14 days. At the end of incubation, the cells were fixed in cold methanol and stained with crystal violet for 30 min. The number of colonies consisting of at least 50 cells was counted.

2.6 | MTT assay

Cells (1×10^4) were seeded in 96-well plates and cultured in a cell incubator at 37°C. At 24, 48, 72, and 96 h, 50 μL MTT solution (KeyGen) was added and incubated for 4 h. After removal of the supernatant, 150 μL DMSO was added, and the absorbance (OD value) was measured at 490 nm. Cells were treated with erastin for 24 h, ferrostatin-1 (Fer-1) for 24 h, MK-2206 for 96 h, and PTX for 48 h. After treatment with these drugs, 50 μL MTT solution was added and incubated for 4 h. Cell viability was calculated using the following equation:

$$\text{Cell viability} = (\text{Mean OD treated} - \text{Mean OD blank})/$$
$$(\text{Mean OD untreated} - \text{Mean OD blank})$$

2.7 | Tubule formation assay

Matrigel (30 μL) was added to a 24-well plate and incubated for 30 min to set the gel. Cells (1.5×10^4) were added to the Matrigel and incubated for 6, 12, and 24 h to observe the tubule formation.

2.8 | Measurement of ROS

Intracellular ROS levels were detected using the fluorescent probe DHE (KeyGen). Cells were seeded in six-well plates, and the probe was added to the medium in the dark. ROS levels were observed by fluorescence microscopy after 40 min of incubation at 37°C.

2.9 | Determination of malondialdehyde (MDA), glutathione, and ferrous iron levels

Detection kits for MDA (Elabscience), GSH (Beyotime), and ferrous ion (Elabscience) were used to assess their cellular content.

2.10 | Xenografts

Four-week-old female BALB/c nude mice (Purchased from Beijing Huafukang Biotechnology Co. LTD) were maintained in laminar flow cabinets and inoculated subcutaneously with a 100-μL suspension of MDA-MB-231 cells (5×10^6). The tumor volume (TV) was calculated using the formula $TV = 1/2 \times a \times b^2$, where a is tumor length and b is tumor width. The mice were sacrificed after 4 weeks, and the xenograft tumors were processed for analysis by immunohistochemistry (IHC).

2.11 | Immunohistochemistry staining and evaluation

Immunohistochemistry staining and evaluation were done following previously reported methods.[17] The evaluation of Ki67 staining was performed at hotspots within the xenograft tissue, with positive signals in nuclei appearing as brown (yellow) granules. Ten microscopic fields were selected for viewing under high power field (×400), with 100 cells counted in each field. The Ki67 index is the percentage of positive cells among the total cells.

2.12 | Transfection and luciferase reporter assays

The HEK293T cell line was transfected with lentivirus packaging GLuc-ON promoter clone GPX4 plasmids (GeneCopoeia). Cells were expanded and transfected using the Lenti-Pac HIV Expression Packing Kit (GeneCopoeia). Cell culture medium was collected and luciferase activity measured using the Secrete-Pair Dual Luminescence Assay Kit (GeneCopoeia).

2.13 | Bioinformatic analysis

The following public databases were searched: TIMER2.0 (http://timer.comp-genomics.org/), Gene Expression Profiling Interactive Analysis 2.0 (GEPIA2) (http://gepia2.cancer-pku.cn/#index), Human Protein Atlas database (https://www.proteinatlas.org), Breast Cancer Gene-Expression Miner v4.9 (bc-GenExMiner v4.9, http://bcgenex.ico.unicancer.fr/BC-GEM/GEM-Accueil.php), Kaplan–Meier (KM) Plotter (http://kmplot.com/analysis/), Genecards database (http://www.genecards.org), National Center for Biotechnology Information (https://www.ncbi.nlm.nih.gov/), Jaspar database (https://jaspar.genereg.net), Xiantao Academic (https://www.xiantao.love/products), Metascape (http://metascape.org/), and Gene Set Enrichment Analysis (GSEA). The GEO database GSE76275 dataset was used to analyze the expression of PTGER3 and GPX4 mRNA in TNBC and non-TNBC, as well as the correlation between the expression of related molecules and PTGER3 in TNBC.

2.14 | Statistical analysis

All statistical calculations were performed using GraphPad Prism (version 5.0). All results were presented as the mean ± standard deviation (SD). Students' t-tests were used to compare the means of two groups, while ANOVA was used to compare the means of multiple groups. $p < 0.05$ was considered to be statistically significant.

3 | RESULTS

3.1 | PTGER3 is low expressed in TNBC and leads to poor prognosis

To explore the possible role of PTGER3 in tumorigenesis, we first analyzed the expression of PTGER3 mRNA in human TCGA cancer tissues within the TIMER2.0 database. As shown in Figure S1A, PTGER3 was expressed at low levels in a variety of cancer types. Similarly, the expression of PTGER3 mRNA and protein in breast cancer was lower than in normal breast tissue (Figure S1B,C). PTGER3 protein was expressed in the plasma membrane and nucleus of normal breast tissue cells (Figure S1C). Analysis of the TIMER2.0 database revealed variable expression of PTGER3 in different molecular subtypes of breast cancer (Figure S1A). Moreover, analysis of 4387 breast cancer cases revealed that PTGER3 expression in basal-like breast cancer tissues was significantly lower than in other molecular subtypes (Figure S1D). Similar results were obtained with the bc-GenExMiner v4.9 database (Figure S1E) and

the GSE76275 dataset (Figure S1F). The prognostic significance of PTGER3 expression in 712 patients with TNBC was evaluated using the bc-GenExMiner v4.9 database (Figure S1G). A significant difference in OS was observed between PTGER3-high- and -low-expression groups, with the low-expression group showing worse survival.

3.2 | Knockdown of PTGER3 promotes the invasion, migration, and proliferation of breast cancer cells

The PTGER3 protein expression level was evaluated in the non-TNBC cell line MCF-7 and in the TNBC cell lines MDA-MB-453 and MDA-MB-231. PTGER3 expression was lowest in MDA-MB-231 and highest in MCF-7 cells (Figure 1A). As shown in Figure S2A, although transfection of sh1-PTGER3 and sh2-PTGER3 plasmids resulted in significant PTGER3 expression inhibition ($p < 0.05$), sh3-PTGER3 did not induce obvious PTGER3 inhibition ($p > 0.05$) after quantitative Western blot analysis (right portion of Figure S2A). Therefore, we chose sh1-PTGER3 and sh2-PTGER3 plasmid for subsequent experiments to rule out off-target effects. Next, we selected stable overexpression and downregulation of PTGER3 in MDA-MB-231 (Figure 1B, Figure S2B) and MCF-7 (Figure 1C, Figure S2B) cells, respectively. Wound-healing assay showed that downregulation of PTGER3 with sh1-PTGER3 and sh2-PTGER3 promoted horizontal migration of MDA-MB-231 and MCF-7 cells (Figure 1D,E, Figure S2C,D). MDA-MB-231-sh-PTGER3 cells showed the fastest migration and almost repaired the wound within 48 h. Migration and invasion assays showed that knockdown of PTGER3 with sh1-PTGER3 and sh2-PTGER3 significantly increased vertical migration and invasion, while PTGER3 overexpression reduced vertical migration and invasion of MDA-MB-231 (Figure 1F, Figure S2E) and MCF-7 (Figure 1G, Figure S2F) cells when compared with control cells.

In addition, colony formation assay showed that MDA-MB-231 sh1-PTGER3 and sh2-PTGER3 cells formed significantly more colonies than control and upregulated cells (Figure 1H, Figure S2I). The same trend was observed in MCF-7 cells (Figure 1I, Figure S2J). Cell proliferation was also evaluated using the MTT assay, which confirmed that loss of PTGER3 expression increased cell proliferation, whereas overexpression of PTGER3 inhibited the proliferation of MDA-MB-231 and MCF-7 cells (Figure 1J,K, Figure S2G,H).

3.3 | Downregulation of PTGER3 enhances epithelial–mesenchymal transition (EMT) in TNBC cells

Western blot analysis showed that upregulation of PTGER3 in MDA-MB-231 cells with an EMT phenotype increased the protein expression of the epithelial marker E-cadherin. Moreover, PTGER3 upregulation inhibited protein expression of the mesenchymal marker vimentin, indicating reversal of the EMT phenotype in MDA-MB-231 cells (Figure 2A). In contrast, PTGER3 knockdown with sh1-PTGER3 and sh2-PTGER3 enhanced the EMT phenotype of MDA-MB-231 cells (Figure 2A, Figure S3A). PTGER3 overexpression or knockdown in MCF-7 cells had no significant effect on the expression of EMT-related markers (Figure 2A, Figure S3A).

Given that PTGER3 affects the EMT phenotype of TNBC cells, not non-TNBC cells, we used the GSE76275 dataset for EMT-related gene expression correlation analysis in TNBC. The data were divided into PTGER3-high- and -low-expression groups according to PTGER3 gene expression. The results showed that the genes in the PTGER3-low-expression group were more involved in the transforming growth factor-β (TGFβ) pathway (Figure 2B). Analysis of EMT-related factors confirmed that PTGER3 expression showed significant negative correlations with CDH2 (Figure 2C) and TFCP2 (Figure 2D) expression, both of which are positive regulators of EMT. Moreover, MDA-MB-231 cells transfected with sh1-PTGER3 and sh2-PTGER3 showed increased mesenchymal morphology, with a more obvious long spindle shape and looser intercellular connections (Figure 2E, Figure S3B, red arrow). In contrast, MDA-MB-231 cells with PTGER3 overexpression showed a more epithelial morphology (Figure 2E, Figure S3B). This phenomenon was not observed with MCF-7 cells (Figure 2F, Figure S3C).

Epithelial–mesenchymal transition often promotes the formation of vasculogenic mimicry (VM) in tumors.[18] Transfection of MDA-MB-231 cells with sh1-PTGER3 and sh2-PTGER3 enhanced their ability to form VM tubules compared with the control group, whereas upregulation of PTGER3 weakened this ability (Figure 2G, Figure S3D). However, the differential expression of PTGER3 in MCF-7 cells had no effect on VM formation ability (Figure 2H, Figure S3E). Western blot analysis showed that expression of matrix metalloproteinase 2 (MMP2), a VM marker, was increased following sh1-PTGER3 and sh2-PTGER3 transfection of MDA-MB-231 cells (Figure 2A, Figure S3A).

3.4 | PTGER3 affects ferroptosis of TNBC cells by targeting GPX4

Our previous study showed that cell death, such as linearly patterned programmed cell necrosis (LPPCN), was associated with VM.[19] We therefore investigated the relationship between PTGER3 expression and LPPCN. As shown in Figure 3A, expression of the LPPCN marker RIPK1 in MDA-MB-231 and MCF-7 cells did not change following alteration of PTGER3 expression. The involvement of PTGER3 during other forms of cell death was also investigated. Interestingly, the ferroptosis marker GPX4 was differentially expressed in MDA-MB-231 cells with altered PTGER3 expression. GPX4 expression was increased in MDA-MB-231 cells with PTGER3 knockdown and decreased in MDA-MB-231 cells that overexpressed PTGER3. These results indicate that GPX4 is a putative downstream effector of PTGER3.
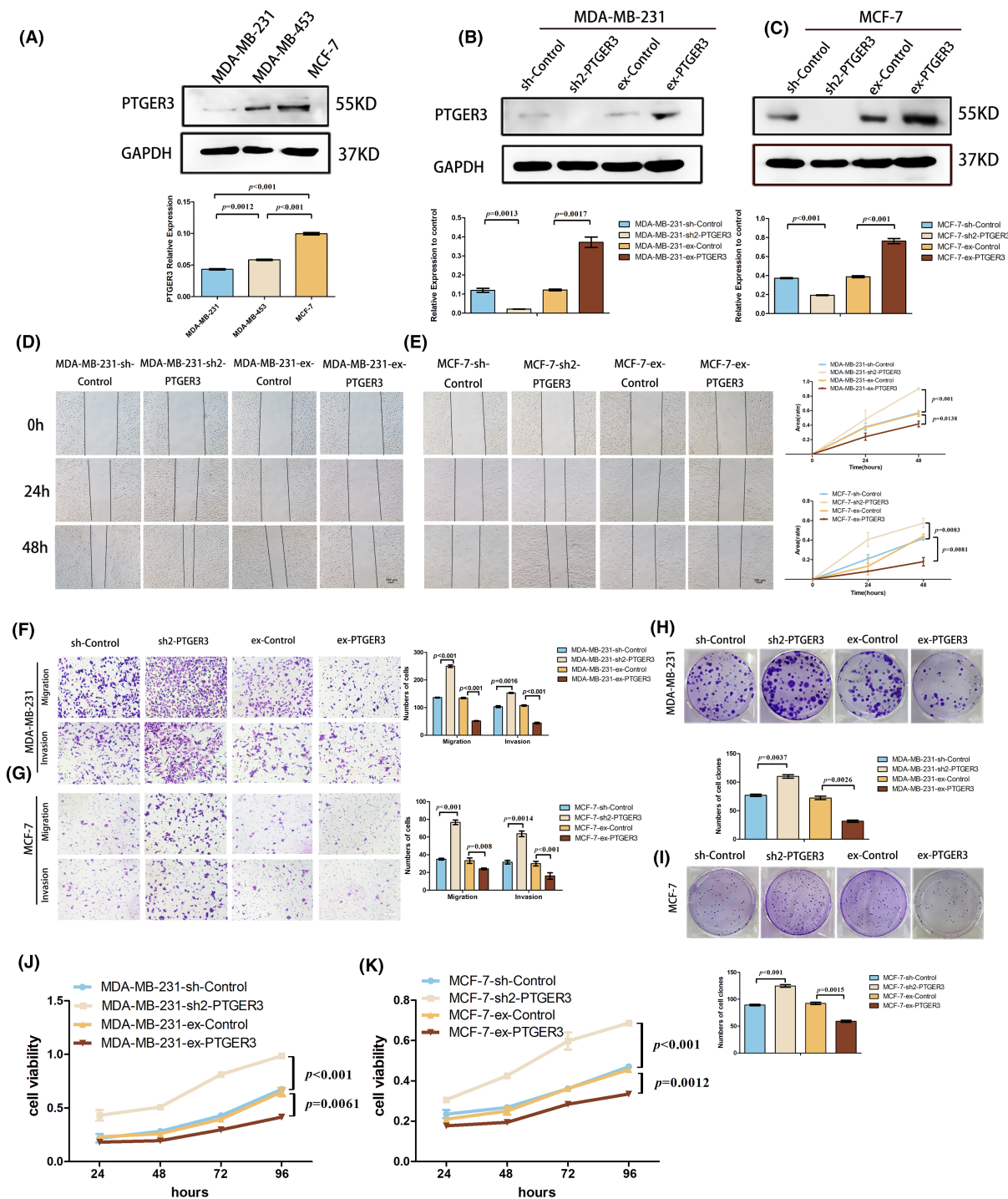
FIGURE 1 Prostaglandin E receptor 3 (PTGER3) knockdown promotes triple-negative breast cancer (TNBC) cell migration, invasion, and proliferation. (A) Western blotting and quantitative analysis showing that PTGER3 expression was relatively low in MDA-MB-231 cells and high in MCF-7 cells. (B, C) Western blot and quantitative analysis showing the expression of PTGER3 in MDA-MB-231 and MCF-7 cells after transfection with the up-/downregulated plasmids. (D, E) Wound-healing assay was performed on MDA-MB-231 and MCF-7 cells with altered PTGER3 expression. Scale bars: 100 μm. (F, G) Migration and invasion assays were performed on MDA-MB-231 and MCF-7 cells with altered PTGER3 expression. Scale bars: 100 μm. (H, I) Colony formation assay was performed on MDA-MB-231 and MCF-7 cells with altered PTGER3 expression. (J, K) MTT assay was performed on MDA-MB-231 and MCF-7 cells with altered PTGER3 expression. Data are presented as the mean ± SD. Student's *t*-test result.

Subcellular analysis of PTGER3 protein showed that it was expressed in the nucleus except plasma membrane (Figures 3B and 4B, Figure S1C). Previous research has focused mainly on the

function of membranous PTGER3 protein,[20–22] with little research so far on the function of nuclear PTGER3. We used the NCBI and JASPAR databases to identify possible binding sites for PTGER3 in
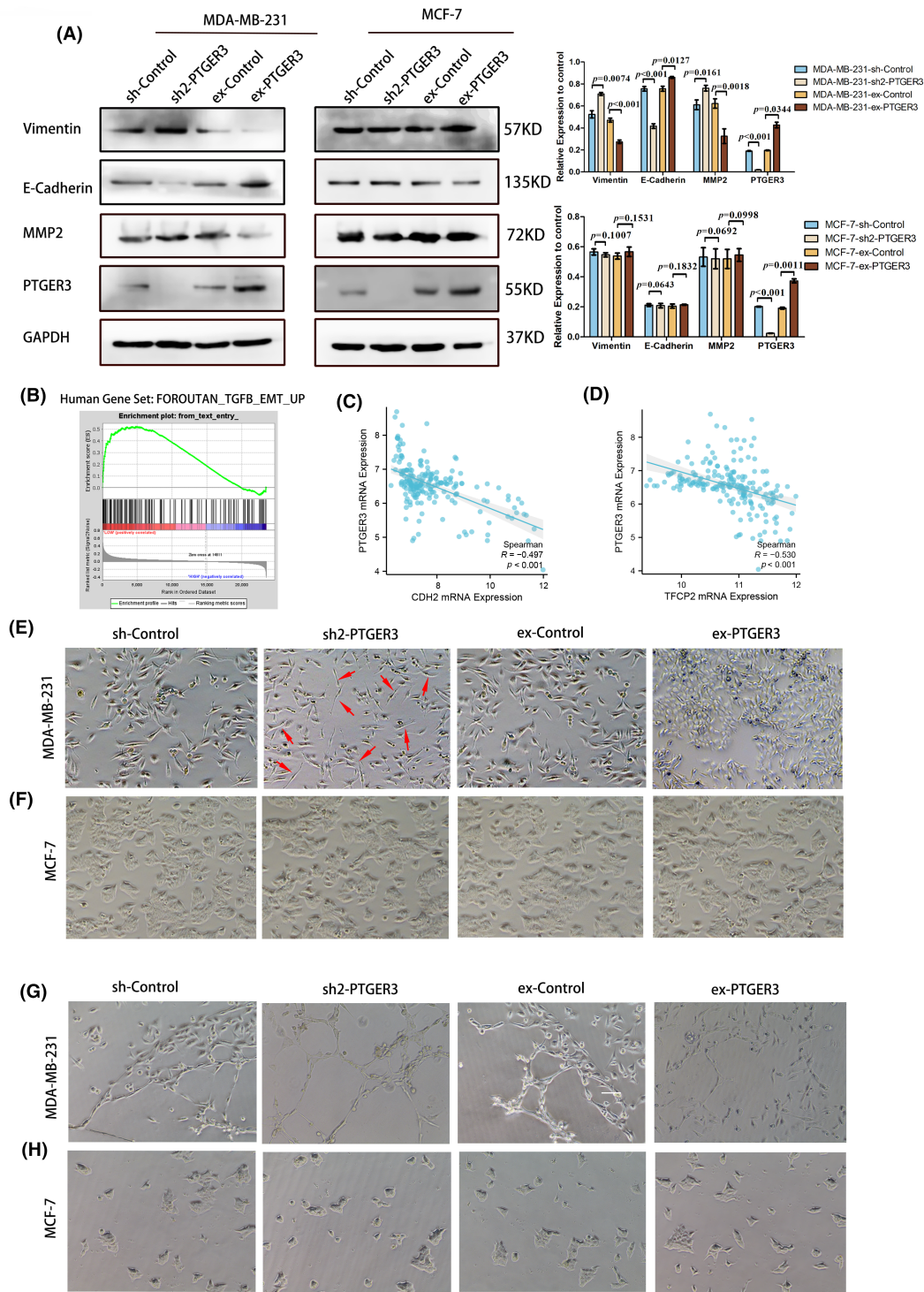
FIGURE 2 Downregulation of prostaglandin E receptor 3 (PTGER3) enhances epithelial–mesenchymal transition (EMT) in triple-negative breast cancer (TNBC) cells. (A) Western blotting was used to assess the protein levels of EMT-related molecules. (B) GSEA analysis showed that low PTGER3 expression was associated with the TGFβ pathway of EMT. (C, D) Analysis of the GSE76275 dataset revealed significant negative correlations between PTGER3 expression and expression of the EMT molecules CDH2 and TFCP2. (E, F) sh2-PTGER3-transfected MDA-MB-231 cells showed more mesenchymal morphology (red arrow), while PTGER3-overexpressing MDA-MB-231 cells showed more epithelial morphology. (G, H) MDA-MB-231 and MCF-7 cells stably transfected with plasmids were used in the tubule formation assay to determine VM formation ability. Data are presented as the mean ± SD. Student's t-test results.

FIGURE 3 Prostaglandin E receptor 3 (PTGER3) affects ferroptosis of triple-negative breast cancer (TNBC) cells by targeting GPX4. (A) Western blotting showing increased GPX4 expression in PTGER3-knockdown MDA-MB-231 cells and decreased GPX4 expression in PTGER3-overexpression MDA-MB-231 cells. RIPK1 expression showed no significant changes. (B) Subcellular localization of PTGER3 expression. (C) PTGER3 binding site sequence as predicted from JASPAR. (D) The luciferase activity of cells cotransfected with the ex-PTEGR3 plasmid and GPX4 promoter was significantly lower compared with other groups. (E) With increasing ex-PTEGR3 plasmid dose, the luciferase activity gradually declined. This dose–response pattern suggests that PTGER3 binds to the GPX4 promoter. (F–M) GSH (F, G), ROS (H, I), MDA (J, K), and ferrous ion (L, M) levels in cells treated with DMSO, erastin, and erastin+Fer-1 (scale bars: 100μm). Data are presented as the mean±SD. One-way ANOVA.
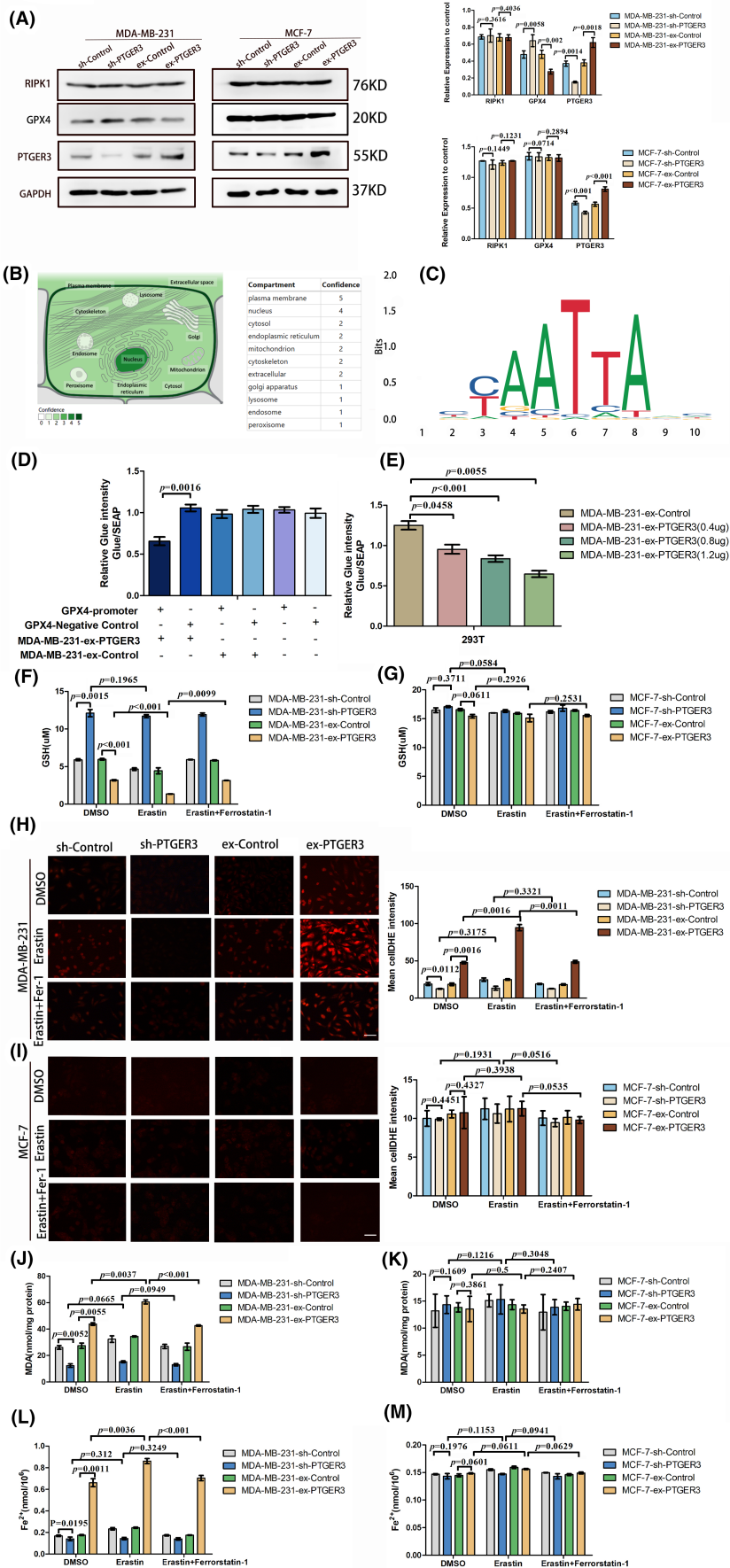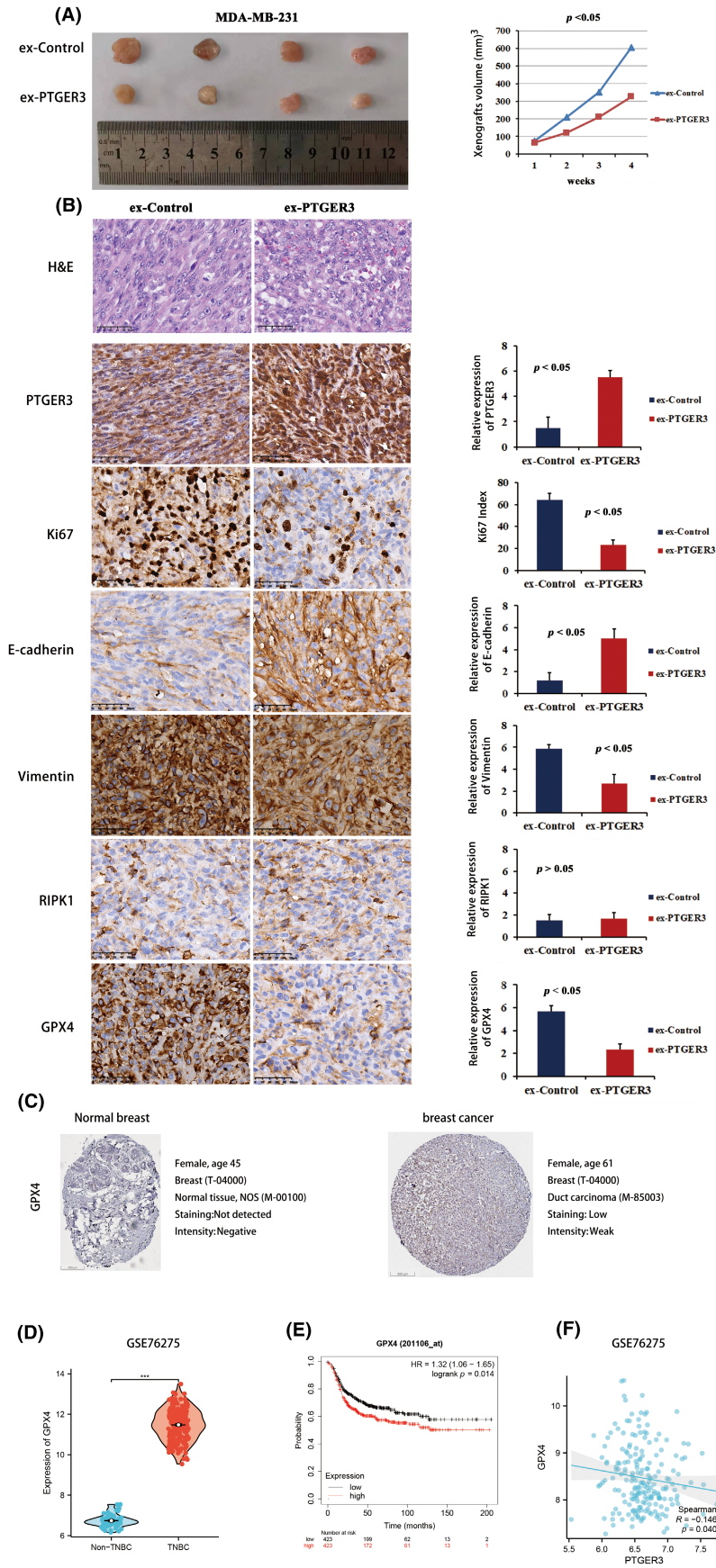
FIGURE 4 Prostaglandin E receptor 3 (PTGER3) affects triple-negative breast cancer (TNBC) cell survival and growth in vivo by affecting ferroptosis. (A) Overexpression of PTGER3 had an inhibitory effect on tumor growth. (B) Hematoxylin–eosin (H&E) staining of the xenografts. Immunohistochemistry (IHC) staining was used to evaluate the expression of PTGER3, Ki67, E-cadherin, vimentin, RIPK1, and GPX4 (scale bars: 50 μm). (C) GPX4 protein expression in breast cancer tissue samples and corresponding noncancer tissue samples (scale bars: 200 μm). (D) Violin plot showing the relative expression of GPX4 in TNBC and non-TNBC tissues from the GSE76275 dataset (***$p < 0.001$). (E) Kaplan–Meier survival curve showing the prognostic value of GPX4 expression in TNBC patients. (F) Significant negative correlation between PTGER3 expression and GPX4 expression in samples from the GSE76275 dataset.

the promoter region of GPX4. Seven putative PTGER3-binding sites with homology >85% were identified in the DNA transcriptional regulatory region of GPX4 (Table S1) (Figure 3C). The PTGER3-binding sites contained a CCAAT sequence that overlapped with a cyclic adenosine monophosphate (cAMP) response element-binding protein (CREB) binding site.[23] We next constructed a GPX4 promoter plasmid containing the above predicted binding site and performed dual luciferase reporter gene experiments to investigate whether PTGER3 expression affected GPX4 promoter activity. The ex-PTEGR3 or ex-control plasmids were cotransfected into 293 T cells together with the GPX4 promoter or negative control plasmids. The luciferase activity in cells cotransfected with ex-PTEGR3 plasmid and GPX4 promoter was significantly lower than in the other groups (Figure 3D) and gradually reduced with increasing doses of ex-PTEGR3 plasmid. This dose–response pattern suggests that PTGER3 can bind to the GPX4 promoter (Figure 3E) to inhibit GPX4 expression.

GPX4 is an important regulator of ferroptosis,[24] with the occurrence of ferroptosis often accompanied by decreased expression of GPX4. Therefore, we hypothesized that differential expression of PTGER3 affects ferroptosis in TNBC cells by regulating GPX4 expression. The level of GSH, a reducing substrate for GPX4 activity, was also examined. Following downregulation of PTGER3 expression in MDA-MB-231 cells, the GSH content increased significantly (Figure 3F). However, the ferroptosis inducer erastin did not cause any change in the GSH level in PTGER3 knockdown MDA-MB-231 cells (Figure 3F). Importantly, the GSH content was significantly lower in MDA-MB-231 cells with upregulated PTGER3. This was amplified by erastin, whereas the ferroptosis inhibitor Fer-1 rescued the above effect (Figure 3F). Similar changes were not observed in MCF-7 cells (Figure 3G).

The basal level of ROS in MDA-MB-231 cells was observed using fluorescence microscopy, which confirmed the sensitivity of TNBC cells to ferroptosis (Figure 3H). The overexpression of PTGER3 increased intracellular ROS levels in MDA-MB-231 cells, whereas knockdown of PTGER3 reduced ROS levels (Figure 3H). Addition of erastin amplified this difference, but the effect was reversed by Fer-1 (Figure 3H). However, there were no significant changes in the ROS level in MCF-7 cells (Figure 3I). Similar trends were observed for lipid peroxides (MDA). The MDA content in MDA-MB-231 cells increased after upregulation of PTGER3 expression and decreased after downregulation of PTGER3 expression, with more pronounced differences after erastin treatment. Treatment with Fer-1 reversed the effect of erastin induction (Figure 3J). No change in the MDA content was observed in MCF-7 cells (Figure 3K).

PTGER3 overexpression in MDA-MB-231 cells markedly increased the intracellular ferrous ion content (Figure 3L). Erastin also significantly increased the ferrous ion content in PTGER3-overexpressing MDA-MB-231 cells, while Fer-1 antagonized this increase (Figure 3L). However, PTGER3 knockdown did not have a significant impact on the ferrous ion content of MDA-MB-231 cells,

even with erastin induction (Figure 3L). MCF-7 cells with altered PTGER3 expression did not show any changes in ferrous ion content (Figure 3M), nor did they show changes related to erastin-induced ferroptosis (Figure 3M).

3.5 | PTGER3 affects TNBC cell survival and growth by impacting ferroptosis

The MTT assay results showed that erastin treatment did not significantly affect the survival of MDA-MB-231 cells with PTGER3 knockdown compared with control cells (Figure S4A). However, the survival rate of MDA-MB-231 cells with PTGER3 overexpression was significantly reduced by erastin. This effect was abolished by Fer-1 (Figure S4B). No significant changes in MCF-7 cell viability were observed following erastin or Fer-1 treatment (Figure S4C,D).

Colony formation assay showed that the growth of MDA-MB-231 cells with PTGER3 knockdown was not affected by erastin treatment (Figure S4E). However, the proliferation of MDA-MB-231 cells with PTGER3 overexpression was significantly inhibited by erastin treatment and the number of colonies was reduced (Figure S4E). These changes were reversed by the addition of Fer-1. The colony formation ability of MCF-7 cells with different PTGER3 expression levels was not affected by either erastin or Fer-1 (Figure S4F).

To investigate the effect of PTGER3 on TNBC progression in vivo, animal experiments were conducted using MDA-MB-231 cells with PTGER3 overexpression, as well as control cells. The tumor growth rate in the group with upregulated PTGER3 was slower than in the control group (Figure 4A). PTGER3 protein expression was increased in MDA-MB-231 PTGER3-upregulated cells, and nuclear PTGER3 expression was dramatically increased compared with control cells (Figure 4B). In addition, the cell proliferation marker Ki67 was lower in the PTGER3-overexpression group (Figure 4B). Moreover, E-cadherin expression was increased in PTGER3-overexpression xenografts, and vimentin expression was decreased (Figure 4B). No significant difference in the expression of RIPK1 was observed between the PTGER3-overexpression and control groups. However, GPX4 expression in the PTGER3-overexpression group was lower than in the control group (Figure 4B).

We next compared GPX4 protein expression between breast cancer and normal breast tissues from the HPA database. GPX4 protein expression was not detected in normal breast tissues, while breast cancer tissues showed weak positive GPX4 expression (Figure 4C). In the GSE76275 dataset, GPX4 expression was higher in TNBC than in non-TNBC (Figure 4D). KM plotter analysis revealed that TNBC patients with high GPX4 expression had poorer prognosis than those with low expression (Figure 4E). Moreover, the negative correlation between GPX4 and PTGER3 expression was confirmed in TNBC (Figure 4F). We conclude from the above results that PTGER3 expression promotes ferroptosis of TNBC cells and inhibits the development of TNBC in vivo.

3.6 | The PI3K-AKT pathway is activated in PTGER3-downregulated TNBC cells

Previous research showed that activation of the PI3K-AKT pathway makes cancer cells more resistant to ferroptosis.[25] GPX4 can interact with the PI3K-AKT downstream effector, the mTOR signaling pathway, and inhibition of GPX4 activity can block mTOR activation in cancer cells.[26] In the present study, the PI3K-AKT pathway in TNBC was found to be closely associated with PTGER3 expression (Figure 5A). This pathway was activated under conditions of low PTGER3 expression (Figure 5B). We also examined the expression and phosphorylation of AKT (p-AKT), a key factor in the PI3K-AKT pathway, in MDA-MB-231 and MCF-7 cells. As shown in Figure 5C, depletion of PTGER3 in MDA-MB-231 cells promoted AKT phosphorylation, whereas PTGER3 overexpression inhibited AKT phosphorylation. No changes in AKT and p-AKT expression were found in MCF-7 cells with altered PTGER3 expression.

In MDA-MB-231 cells with altered PTGER3 expression, p-AKT expression was decreased after adding the AKT inhibitor MK-2206 (Figure 5D). Interestingly, GPX4 protein expression did not alter significantly after the addition of MK-2206 (Figure 5D). However, the GSH content was significantly decreased in PTGER3-downregulated MDA-MB-231 cells after treatment with MK-2206. This decrease was greater after cotreatment with erastin but was reversed by Fer-1 (Figure 5E). MK-2206 had no significant effect on the GSH content of MDA-MB-231 cells with upregulated PTGER3 (Figure 5E). The GSH content of MCF-7 cells was not affected by MK-2206 either (Figure 5F). PI3K-AKT activation could stimulate GSH biosynthesis in mammary epithelial cells by stabilizing and activating Nrf2 to upregulate GSH biosynthetic genes, and elevated GSH biosynthesis is required for PI3K-AKT-driven resistance to oxidative stress.[27] Consistent with this earlier study, our results showed that inhibition of the PI3K-AKT pathway significantly decreased the GSH level, thereby inducing ferroptosis in MDA-MB-231 cells with PTGER3 knockdown.

Of note, erastin caused the ROS content to increase in all MDA-MB-231 cells, including those with PTGER3 knockdown after the addition of MK-2206 (Figure 5G) and those which had been antagonized by Fer-1. This demonstrates that inhibition of the PI3K-AKT pathway recovered the sensitivity of MDA-MB-231 cells with PTGER3 knockdown to ferroptosis. In contrast to MDA-MB-231 cells, the level of ROS in MCF-7 cells did not show any significant changes in response to treatment with MK-2206 or to MK-2206 combined with erastin (Figure 5H).

Neither MK-2206 alone or in combination with erastin affected the MDA level (Figure S5A) or the ferrous ion content (Figure S5C) in MDA-MB-231 cells with PTGER3 knockdown. However, the MDA and ferrous ion content of MDA-MB-231 cells with PTGER3 overexpression increased after MK-2206 treatment, and even more so after cotreatment with erastin. The MDA and ferrous ion content decreased after Fer-1 treatment, suggesting the existence of other MK-2206-induced mechanisms of ferroptosis in PTGER3-overexpressing MDA-MB-231 cells in addition to inhibition of the

PI3K-AKT pathway. MK-2206 did not induce any changes in the MDA or ferrous ion content of MCF-7 cells (Figure S5B,D).

MTT assay and colony formation assay revealed the proliferation and clonality of PTGER3-knockdown MDA-MB-231 cells were both inhibited by MK-2206 (Figure S5E,I). This inhibitory effect was even greater in combination with erastin but was reduced by Fer-1 (Figure S5E,I). MK-2206 had no significant inhibitory effect on the cell viability and clonality of MDA-MB-231 cells with upregulated PTGER3 (Figure S5F,I). No differences were observed in MCF-7 cells (Figure S5G,H,J).

3.7 | PTGER3 overexpression enhances the sensitivity of TNBC cells to paclitaxel (PTX)

Treatment of PTGER3-overexpressing MDA-MB-231 cells with PTX significantly increased the levels of ROS (Figure S6A), MDA (Figure S6C), and ferrous ion (Figure S6E) and decreased the GSH content (Figure S6G) compared with control cells. This result suggests that overexpression of PTGER3 could enhance the sensitivity of TNBC cells to PTX through the induction of ferroptosis. The effect was more pronounced by the addition of erastin and was counteracted by Fer-1 (Figure S6A,C,E,G). However, PTX had little effect on the ROS, MDA, GSH, and ferrous ion contents of MDA-MB-231 cells with PTGER3 knockdown (Figure S6A,C,E,G), or MCF-7 cells (Figure S6B,D,F,H).

We further investigated the effect of PTX on cell proliferation and clonality in MDA-MB-231 and MCF-7 cells with altered PTGER3 expression. PTX did not affect the proliferation and clonality of MDA-MB-231 cells with downregulated PTGER3 (Figure 6A,E). However, it significantly inhibited the proliferation of MDA-MB-231 cells with upregulated PTGER3 and decreased the number of colonies. The combination of PTX and erastin had the strongest inhibitory effect on the cell viability and clonality of MDA-MB-231 cells with upregulated PTGER3, which was attenuated by treatment with Fer-1 (Figure 6B,E). PTX did not affect the proliferation ability and clonality of MCF-7 cells (Figure 6C,D,F).

4 | DISCUSSION

Triple-negative breast cancer is the most lethal subtype of breast cancer and is characterized by high heterogeneity, aggressiveness, and lack of effective treatment options.[28] Furthermore, TNBC is not sensitive to targeted and endocrine therapy and is highly resistant to chemotherapy.[29] Hence, there is an urgent need to find effective treatments for TNBC.

PGE2 is a major COX-2 metabolite and is abundant in the cancer microenvironment. It exerts multiple effects through four G protein-coupled receptors designated as PTGER1-4 and through corresponding downstream pathways. PGE2 is positively correlated with ferroptosis, and the inhibition of ferroptosis induced by cerebral ischemia reperfusion can inactivate the COX-2/PGE2 pathway,

FIGURE 5 Activation of the PI3K-AKT pathway in prostaglandin E receptor 3 (PTGER3)-downregulated triple-negative breast cancer (TNBC) cells. (A) KEGG pathway enrichment of PTGER3-related genes identified the PI3K-AKT pathway as the top-ranked pathway. (B) GSEA analysis showed that low PTGER3 expression was closely associated with the PI3K-AKT pathway. (C) Western blotting showed that PTGER3 knockdown promoted AKT phosphorylation in MDA-MB-231 cells, whereas PTGER3 overexpression inhibited AKT phosphorylation. (D) Following the addition of MK-2206 to MDA-MB-231 cells with altered PTGER3 expression, the expression of p-AKT decreased, but GPX4 expression did not change significantly. (E, F) Evaluation of GSH content in cells after different treatments. (G, H) Quantitative analysis using the DHE probe to determine reactive oxygen species (ROS) levels in cells after different treatments (erastin: 2 μM; MK-2206: 5 μM; Fer-1: 5 μM) Scale bars: 100 μm. Data are presented as the mean ± SD. One-way ANOVA.
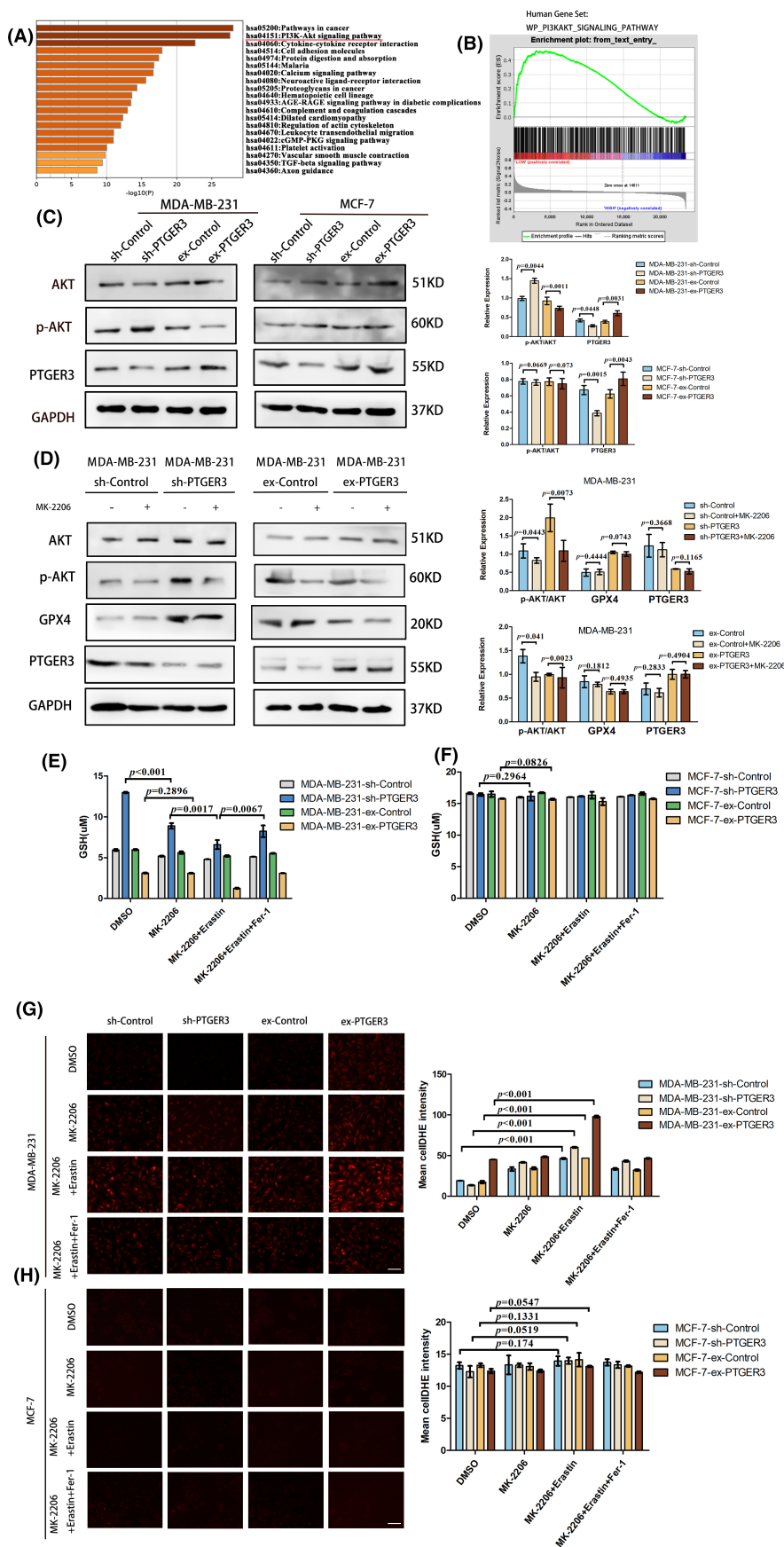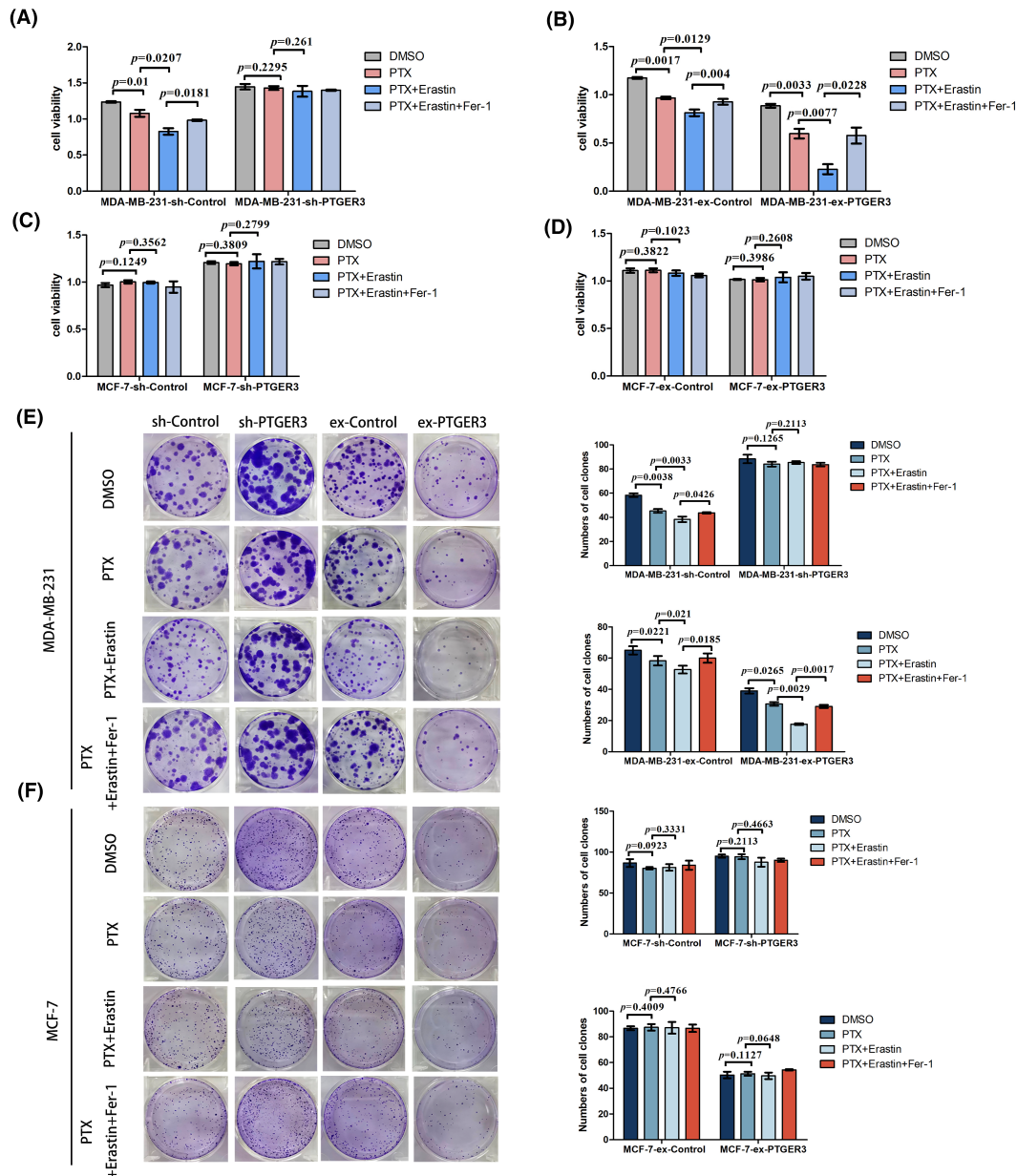
FIGURE 6 Triple-negative breast cancer (TNBC) cells with prostaglandin E receptor 3 (PTGER3) overexpression showed increased sensitivity to paclitaxel (PTX) and inhibition of cell proliferation. (A–D) MTT assay was used to determine the effect of PTX and PTX+erastin on the proliferation of MDA-B-231 cells (A, B) and MCF-7 cells (C, D) with altered PTGER3 expression. (E, F) Colony formation assay was used to evaluate the effect of PTX and PTX+erastin on the colony-forming ability of MDA-MB-231 cells (E) and MCF-7 cells (F) with altered PTGER3 expression (erastin: 2 μM; PTX: 0.25 μM; Fer-1: 5 μM). Data are presented as the mean±SD. One-way ANOVA.

possibly via PTGER3/4.[20] Excessive accumulation of PGE2 can promote ferroptosis during acute kidney injury, while decreased levels of PTGER1/3 can partially restore the decline in GSH and GPX4 levels and inhibit ferroptosis.[21]

PTGER3 is the only prostanoid receptor that couples Gi and functions in a cAMP-inhibitory manner. Sanchez et al. found that PTGER3 can promote p21 expression by reducing cAMP, thereby arresting the cell cycle in the S phase.[22] In hepatocellular carcinoma, CREB was shown to regulate transcription coactivator 3 to protect tumor cells from drug-induced ferroptosis.[30] Hattori et al.[31] and Speckman et al.[32] reported the CCAAT sequence in GPX4 DNA transcriptional

regulatory regions overlapped with a CREB binding site. CREB binds to this CCAAT sequence to upregulate the expression of GPX4 in human lung adenocarcinoma cells and neutrophils, thus inhibiting ferroptosis.[23,33] The present study found that PTGER3 expression affected the migration, invasion, proliferation, and clonality of breast cancer cells. We also found that overexpression of PTGER3 promotes ferroptosis of TNBC cells, possibly by inhibiting a cAMP-dependent pathway and inactivating CREB, thereby reducing the expression of GPX4. In addition, our study further demonstrated that PTGER3 protein was localized in the nucleus where it can bind directly to the GPX4 promoter region and inhibit GPX4 expression.

The GPX4/GSH axis is the most frequently targeted pathway that triggers the ferroptosis cascade.[34] During the process of ferroptosis, GPX4 converts GSH to oxidized glutathione (GSSG) and reduces cytotoxic lipid peroxides (L-OOH) to their corresponding alcohols (L-OH).[35] In our study, GSH content was decreased in PTGER3-overexpression TNBC cells which showed decreased GPX4 expression. ROS, MDA, and ferrous ion levels were increased, which meant the ferroptosis of TNBC cells was increased after the overexpression of PTGER3. Erastin also induced ferroptosis in PTGER3-overexpressing TNBC cells by GPX4 inactivation through depletion of GSH. Importantly, PTGER3 knockdown reduced ferroptosis in TNBC cells by removing the inhibitory effect on GPX4 expression, with erastin treatment being unable to induce ferroptosis in these cells (Figure 7). Of note, we found that PTER3 expression had no significant effect on ferroptosis in non-TNBC cells. Timmermann et al. previously reported that TNBC cells consumed more glutamine than non-TNBC cells and showed intracellular ROS accumulation,[36] thus making them more sensitive to ferroptosis than non-TNBC cells. Zhang et al. recently found that MDA-MB-231 and MCF-7 cells showed different iron homeostasis regulation and redox balance capacity, resulting in higher sensitivity to ferroptosis by MDA-MB-231 cells.[37] Our results are consistent with these findings. Moreover, we observed that overexpression of PTGER3 in MDA-MB-231 cells, not in MCF-7 cells, induced GSH depletion and resulted in TNBC cells being specifically more sensitive to ferroptosis.

Recent studies have demonstrated an interplay between GPX4 expression and the PI3K-AKT-mTOR pathway.[25,26,38] The combination of a PI3K-AKT-mTOR pathway inhibitor and a ferroptosis inducer was shown to eliminate breast cancer BT474 cells and prostate cancer PC-3 cells in mice.[25] In the present study, we showed for the first time that loss of PTGER3 expression in TNBC cells plays a significant role in activating the PI3K-AKT pathway via GPX4 expression. We also demonstrated that abnormal activation of the PI3K-AKT pathway could inhibit ferroptosis of TNBC cells. PI3K-AKT pathway inhibitor can inhibit GSH biosynthesis[27] and inactivate GPX4 in PTGER3-downregulated TNBC cells, thereby inducing ferroptosis (Figure 7).

The PI3K-AKT pathway is one of the most frequently aberrant pathways in TNBC,[39] with activation of the PI3K/AKT/GSK3β axis also being a central feature of EMT. Constitutive activation of PI3K-AKT leads to the repression of epithelial characteristics and increased mesenchymal protein expression.[40] It is well known that EMT can promote tumor progression and drug resistance.[41–43] Colorectal cancer cells with high PTGER3 expression showed EMT-induced progressive cancer, activation of the TGFβ pathway, activation of hypoxia-inducible factor-1α, and suppression of runt-related transcription factor 3.[44] In our study, we also found that low PTGER3 expression was associated with activation of the TGFβ and PI3K-AKT pathways, which may enhance EMT in TNBC.

Paclitaxel chemotherapy regimens have been widely used in patients with TNBC.[45] However, many patients develop drug resistance during the course of long-term treatment, which reduces the treatment effect and leads to disease stress.[46] In the present study of TNBC cells with PTGER3 overexpression, PTX was found to increase the ROS, MDA, and ferrous ion content and to decrease the GSH content, which in turn induced ferroptosis. Moreover, PTGER3 knockdown in TNBC cells decreased PTX-induced ferroptosis. Importantly, the destructive effect of PTX on TNBC cells with
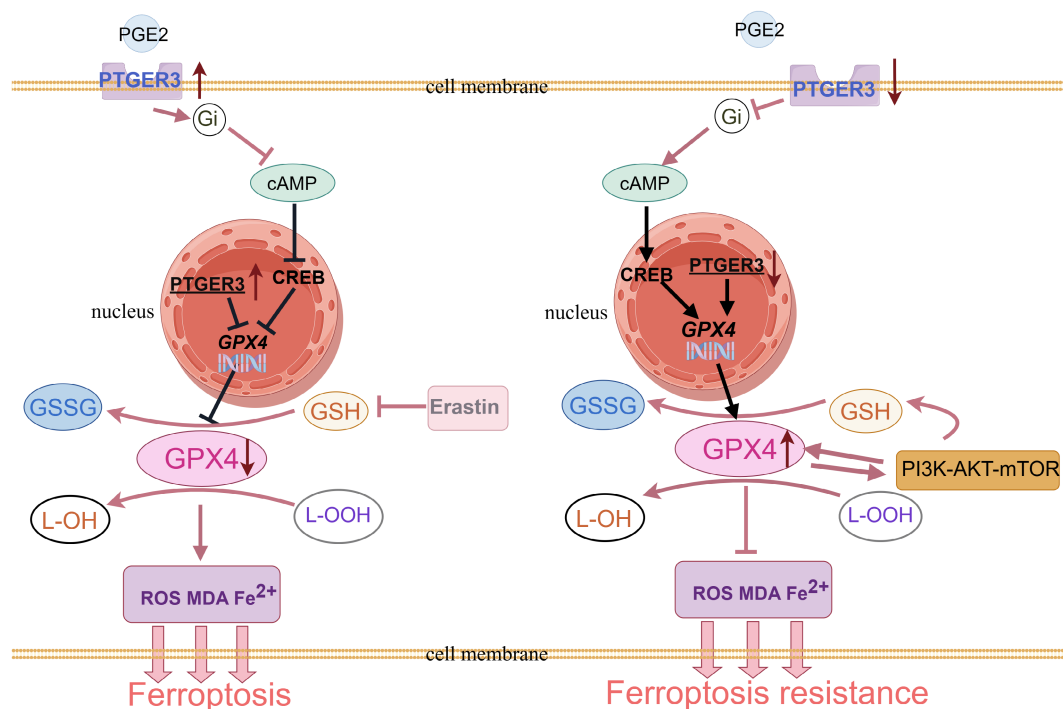

FIGURE 7 Schematic of the proposed mechanism by which the PTGER3-GPX4/GSH-PI3K-AKT axis affects ferroptosis in triple-negative breast cancer (TNBC) (by Figdraw).

PTGER3 overexpression was greater in combination with ferroptosis inducers. Therefore, the best effect of PTX and ferroptosis inducer combination therapy is achieved in TNBC cells with high PTGER3 expression. The loss of PTGER3 expression in TNBC may be related to PTX resistance.

AUTHOR CONTRIBUTIONS

Song Wang: Writing – original draft. **Yueyao Zhang:** Data curation. **Dan Zhang:** Methodology. **Na Che:** Formal analysis. **Jie Meng:** Validation. **Xiulan Zhao:** Writing – review and editing. **Tieju Liu:** Writing – review and editing.

ACKNOWLEDGMENTS

FUNDING INFORMATION

CONFLICT OF INTEREST STATEMENT

The authors declare no conflict of interest.

ETHICS STATEMENT

Approval of the research protocol by an Institutional Reviewer Board: N/A.

Informed Consent: N/A.

Registry and the Registration No. of the study/trial: N/A.

Animal Studies: The study was conducted according to the guidelines of the Declaration of Helsinki and approved by the Animal Research Ethics Committee of Tianjin Medical University.

ORCID

Tieju Liu 🔘 https://orcid.org/0000-0003-4522-545X

REFERENCES

1. Wolff AC, Hammond ME, Hicks DG, et al. Recommendations for human epidermal growth factor receptor 2 testing in breast cancer: American Society of Clinical Oncology/College of American Pathologists clinical practice guideline update. *J Clin Oncol.* 2013;31(31):3997-4013.
2. Dent R, Trudeau M, Pritchard KI, et al. Triple-negative breast cancer: clinical features and patterns of recurrence. *Clin Cancer Res.* 2007;13(15 Pt 1):4429-4434.
3. Chang-Qing Y, Jie L, Shi-Qi Z, et al. Recent treatment progress of triple negative breast cancer. *Prog Biophys Mol Biol.* 2020;151:40-53.
4. Zhai Q, Li H, Sun L, Yuan Y, Wang X. Identification of differentially expressed genes between triple and non-triple-negative breast cancer using bioinformatics analysis. *Breast Cancer.* 2019;26(6):784-791.
5. Cheuk IW, Shin VY, Siu MT, et al. Association of EP2 receptor and SLC19A3 in regulating breast cancer metastasis. *Am J Cancer Res.* 2015;5(11):3389-3399.
6. Semmlinger A, von Schoenfeldt V, Wolf V, et al. EP3 (prostaglandin E2 receptor 3) expression is a prognostic factor for progression-free

7. Zehni AZ, Jeschke U, Hester A, et al. EP3 is an independent prognostic marker only for unifocal breast cancer cases. *Int J Mol Sci.* 2020;21(12):4418.
8. Tang D, Chen X, Kang R, Kroemer G. Ferroptosis: molecular mechanisms and health implications. *Cell Res.* 2021;31(2):107-125.
9. Viswanathan VS, Ryan MJ, Dhruv HD, et al. Dependency of a therapy-resistant state of cancer cells on a lipid peroxidase pathway. *Nature.* 2017;547(7664):453-457.
10. Hangauer MJ, Viswanathan VS, Ryan MJ, et al. Drug-tolerant persister cancer cells are vulnerable to GPX4 inhibition. *Nature.* 2017;551(7679):247-250.
11. Tsoi J, Robert L, Paraiso K, et al. Multi-stage differentiation defines melanoma subtypes with differential vulnerability to drug-induced iron-dependent oxidative stress. *Cancer Cell.* 2018;33(5):890-904 e895.
12. Sun LL, Linghu DL, Hung MC. Ferroptosis: a promising target for cancer immunotherapy. *Am J Cancer Res.* 2021;11(12):5856-5863.
13. Stockwell BR, Jiang X. The chemistry and biology of ferroptosis. *Cell Chem Biol.* 2020;27(4):365-375.
14. Verma N, Vinik Y, Saroha A, et al. Synthetic lethal combination targeting BET uncovered intrinsic susceptibility of TNBC to ferroptosis. *Sci Adv.* 2020;6(34):eaba8968.
15. Doll S, Proneth B, Tyurina YY, et al. ACSL4 dictates ferroptosis sensitivity by shaping cellular lipid composition. *Nat Chem Biol.* 2017;13(1):91-98.
16. Yao X, Xie R, Cao Y, et al. Simvastatin induced ferroptosis for triple-negative breast cancer therapy. *J Nanobiotechnology.* 2021;19(1):311.
17. Li F, Sun H, Yu Y, et al. RIPK1-dependent necroptosis promotes vasculogenic mimicry formation via eIF4E in triple-negative breast cancer. *Cell Death Dis.* 2023;14(5):335.
18. Liu Q, Qiao L, Liang N, et al. The relationship between vasculogenic mimicry and epithelial-mesenchymal transitions. *J Cell Mol Med.* 2016;20(9):1761-1769.
19. Zhang S, Li M, Zhang D, et al. Hypoxia influences linearly patterned programmed cell necrosis and tumor blood supply patterns formation in melanoma. *Lab Investig.* 2009;89(5):575-586.
20. Xu Y, Liu Y, Li K, et al. COX-2/PGE2 pathway inhibits the ferroptosis induced by cerebral ischemia reperfusion. *Mol Neurobiol.* 2022;59(3):1619-1631.
21. Liu Y, Zhou L, Lv C, et al. PGE2 pathway mediates oxidative stress-induced ferroptosis in renal tubular epithelial cells. *FEBS J.* 2023;290(2):533-549.
22. Sanchez T, Moreno JJ. GR 63799X, an EP3 receptor agonist, induced S phase arrest and 3T6 fibroblast growth inhibition. *Eur J Pharmacol.* 2006;529(1–3):16-23.
23. Ursini F, Bosello Travain V, Cozza G, et al. A white paper on phospholipid hydroperoxide glutathione peroxidase (GPx4) forty years later. *Free Radic Biol Med.* 2022;188:117-133.
24. Yang WS, SriRamaratnam R, Welsch ME, et al. Regulation of ferroptotic cancer cell death by GPX4. *Cell.* 2014;156(1–2):317-331.
25. Yi J, Zhu J, Wu J, Thompson CB, Jiang X. Oncogenic activation of PI3K-AKT-mTOR signaling suppresses ferroptosis via SREBP-mediated lipogenesis. *Proc Natl Acad Sci USA.* 2020;117(49):31189-31197.
26. Sekhar KR, Hanna DN, Cyr S, et al. Glutathione peroxidase 4 inhibition induces ferroptosis and mTOR pathway suppression in thyroid cancer. *Sci Rep.* 2022;12(1):19396.
27. Lien EC, Lyssiotis CA, Juvekar A, et al. Glutathione biosynthesis is a metabolic vulnerability in PI(3)K/Akt-driven breast cancer. *Nat Cell Biol.* 2016;18(5):572-578.
28. Nedeljkovic M, Damjanovic A. Mechanisms of chemotherapy resistance in triple-negative breast cancer-how we can rise to the challenge. *Cells.* 2019;8(9):957.

and overall survival in sporadic breast cancer. *BMC Cancer.* 2018;18(1):431.

29. Garrido-Castro AC, Lin NU, Polyak K. Insights into molecular classifications of triple-negative breast cancer: improving patient selection for treatment. *Cancer Discov*. 2019;9(2):176-198.

30. Li L, Xing T, Chen Y, et al. In vitro CRISPR screening uncovers CRTC3 as a regulator of IFN-gamma-induced ferroptosis of hepatocellular carcinoma. *Cell Death Dis*. 2023;9(1):331.

31. Hattori H, Imai H, Kirai N, et al. Identification of a responsible promoter region and a key transcription factor, CCAAT/enhancer-binding protein epsilon, for up-regulation of PHGPx in HL60 cells stimulated with TNF alpha. *Biochem J*. 2007;408(2):277-286.

32. Speckmann B, Bidmon HJ, Pinto A, Anlauf M, Sies H, Steinbrenner H. Induction of glutathione peroxidase 4 expression during enterocytic cell differentiation. *J Biol Chem*. 2011;286(12):10764-10772.

33. Wang Z, Zhang X, Tian X, et al. CREB stimulates GPX4 transcription to inhibit ferroptosis in lung adenocarcinoma. *Oncol Rep*. 2021;45(6):88.

34. Shi Z, Naowarojna N, Pan Z, Zou Y. Multifaceted mechanisms mediating cystine starvation-induced ferroptosis. *Nat Commun*. 2021;12(1):4792.

35. Li J, Cao F, Yin HL, et al. Ferroptosis: past, present and future. *Cell Death Dis*. 2020;11(2):88.

36. Timmerman LA, Holton T, Yuneva M, et al. Glutamine sensitivity analysis identifies the xCT antiporter as a common triple-negative breast tumor therapeutic target. *Cancer Cell*. 2013;24(4):450-465.

37. Zhang Z, Lu M, Chen C, et al. Holo-lactoferrin: the link between ferroptosis and radiotherapy in triple-negative breast cancer. *Theranostics*. 2021;11(7):3167-3182.

38. Cai JY, Ye Z, Hu YY, et al. Fatostatin induces ferroptosis through inhibition of the AKT/mTORC1/GPX4 signaling pathway in glioblastoma. *Cell Death Dis*. 2023;14(3):211.

39. Pascual J, Turner NC. Targeting the PI3-kinase pathway in triple-negative breast cancer. *Ann Oncol*. 2019;30(7):1051-1060.

40. Guo C, Li S, Liang A, Cui M, Lou Y, Wang H. PPA1 promotes breast cancer proliferation and metastasis through PI3K/AKT/GSK3beta signaling pathway. *Front Cell Dev Biol*. 2021;9:730558.

41. Mitra A, Mishra L, Li S. EMT, CTCs and CSCs in tumor relapse and drug-resistance. *Oncotarget*. 2015;6(13):10697-10711.

42. Heerboth S, Housman G, Leary M, et al. EMT and tumor metastasis. *Clin Transl Med*. 2015;4:6.

43. Brabletz T, Kalluri R, Nieto MA, Weinberg RA. EMT in cancer. *Nat Rev Cancer*. 2018;18(2):128-134.

44. Fukushima K, Fujino H. Identification and characterization of human colorectal cancer cluster predominantly expressing EP3 Prostanoid receptor subtype. *Biol Pharm Bull*. 2022;45(6):698-702.

45. Mustacchi G, De Laurentiis M. The role of taxanes in triple-negative breast cancer: literature review. *Drug Des Devel Ther*. 2015;9:4303-4318.

46. Schettini F, Giuliano M, De Placido S, et al. Nab-paclitaxel for the treatment of triple-negative breast cancer: rationale, clinical data and future perspectives. *Cancer Treat Rev*. 2016;50:129-141.

SUPPORTING INFORMATION

Additional supporting information can be found online in the Supporting Information section at the end of this article.